Inorg. Chem. **2008**, *47*, 5815−5820

4-Thiolatobenzoate-Bridged Gold/Zirconium Complex and Its Mononuclear Precursors

Ulrike Helmstedt,[†] Sergei Lebedkin,[‡] Thomas Höcher,[†,§] Steffen Blaurock,[†,§] and E. Hey-Hawkins*[,†]

Institut für Anorganische Chemie, Universität Leipzig, Johannisallee 29, D-04103 Leipzig, Germany, and Institut für Nanotechnologie, Forschungszentrum Karlsruhe, D-76021 Karlsruhe, Germany

Received February 1, 2008

The selective synthesis of a Au^{I} complex of 4-mercaptobenzoic acid, namely, [Au(SC_6H_4-4-COOH)(PMe_2Ph)] (**1**), is reported. It shows interesting photoluminescence (PL) properties, for example, high PL quantum yield, multicomponent emission, and an unusually large PL lifetime. This complex was further applied as a metalloligand for the synthesis of [$Cp^*_2Zr\{\kappa^1O$-$OOCC_6H_4$-4-$SAu(PMe_2Ph)\}\{\kappa^2O,O'$-$OOCC_6H_4$-4-$SAu(PMe_2Ph)\}$] (**3**), one of the rare Au^{I}/Zr^{IV} complexes. For the first time the exchange between the two ligands, which are bound in mono- and bidentate fashion, respectively, could be observed with the help of variable-temperature NMR spectroscopy. For the corresponding monometallic zirconocene complex [$Cp^*_2Zr(\kappa^1O$-$O_2CC_6H_4$-4-SH)(κ^2O,O'-$O_2CC_6H_4$-4-SH)] (**2**) the activation parameters of this exchange could be determined by line shape analysis.

Introduction

Interest in early/late heterobimetallics (ELHBs) has increased in the last decades,[1] as these complexes have proved to be useful in elucidating the mechanisms of enzymes whose active centers include more than one metal atom.[2] They have been utilized in explaining the strong metal−support interaction (SMSI) phenomenon in heterogeneous catalysis,[3] and they are of interest as catalysts[4] and magnetic materials[5] because of cooperative effects between different metal centers. The synthesis of ELHBs preferably starts with the preparation of a monometallic complex, which is then employed as a so-called metalloligand to coordinate to a second metal center. Different concepts for selective coordination of the first metal center by one donor group of a di- or multifunctional ligand are known, for example, exploitation of the chelate effect[6] or the use of donor atoms with different coordination behavior[7] according to the hard and soft acids and bases (HSAB) concept of Pearson.[8]

Applying Pearson's concept we used anions of various aliphatic mercaptocarboxylic acids, such as dianions of mercaptoacetic and mercaptopropionic acid, as bridging ligands between different metal centers and thus obtained dinuclear Mo^{IV}/Zr^{IV}, trinuclear Au^{I}/Zr^{IV}, tetranuclear Ni^{II}/Zr^{IV}, and octanuclear Pd^{II}/Zr^{IV} complexes.[9]

To extend these investigations to nonchelating ligands, we employed the dianion of 4-mercaptobenzoic acid (H_2mba) as bridging ligand. In recent studies dealing with Rh^{I}/Zr^{IV} complexes of H_2mba we showed that this bridge inhibits chelation (because of its rigid carbon backbone) and is

* To whom correspondence should be addressed. E-mail: hey@rz.uni-leipzig.de.
† Universität Leipzig.
‡ Forschungszentrum Karlsruhe.
§ Crystal structure determinations.

(1) Stephan, D. W. *Coord. Chem. Rev.* **1989**, *95*, 41–107.
(2) Holm, R. H.; Kennepohl, P.; Solomon, E. I. *Chem. Rev.* **1996**, *96*, 2239–2314.
(3) Tauster, S. J. *Acc. Chem. Res.* **1987**, *20*, 389–394.
(4) (a) Rida, M. A.; Smith, A. K. *Modern Coordination Chemistry−The Legacy of J. Chatt* Leigh, J. J., Winterton, N., Eds.; Royal Society of Chemistry: Cambridge, U.K., 2002; pp 154−161. (b) Senocq, F.; Randrianalimanana, C.; Thorez, A.; Kalck, P.; Choukroun, R.; Gervais, D. *J. Chem. Soc., Chem. Commun.* **1984**, 1376–1377. (c) Choukroun, R.; Gervais, D.; Jaud, J.; Kalck, P.; Senocq, F. *Organometallics* **1986**, *5*, 67–71. (d) Partenheimer, W.; Amoco Corp. Production of polycarboxylic acids with a molybdenum-activated cobalt catalyst. U.S. Patent US4992580, 1991.
(5) Kahn, O. *Adv. Inorg. Chem.* **1995**, *43*, 179–259.
(6) Fritzsche, S.; Lönnecke, P.; Höcher, T.; Hey-Hawkins, E. *Z. Anorg. Allg. Chem.* **2006**, *632*, 2256–2267.
(7) Ruiz, R.; Faus, J.; Lloret, F.; Julve, M.; Journaux, Y. *Coord. Chem. Rev.* **1999**, *193−195*, 1069–1117.
(8) Pearson, R. G. *Chemical Hardness−Application From Molecules to Solids*; Wiley-VCH: Weinheim, 1997.
(9) (a) Wenzel, B.; Lönnecke, P.; Hey-Hawkins, E. *Z. Anorg. Allg. Chem.* **2003**, *629*, 1596–1600. (b) Wenzel, B.; Lönnecke, P.; Hey-Hawkins, E. *Eur. J. Inorg. Chem.* **2002**, 1761–1764. (c) Wenzel, B.; Lönnecke, P.; Stender, M.; Hey-Hawkins, E. *Z. Anorg. Allg. Chem.* **2002**, *628*, 1925–1929. (d) Wenzel, B.; Lönnecke, P.; Stender, M.; Hey-Hawkins, E. *J. Chem. Soc., Dalton Trans.* **2002**, 478–480. (e) Wenzel, B.; Lönnecke, P.; Hey-Hawkins, E. *Organometallics* **2002**, *21*, 2070–2075.

10.1021/ic800203y CCC: $40.75
Published on Web 06/05/2008

therefore suitable for selective coordination of each functional group to only one metal center.[10] Because of the lability of the rhodium−phosphine bond and the nucleophilicity of the nonbonding electron pairs at sulfur, macrocyclic structures were obtained.[11]

We now show that replacement of rhodium(I) by gold(I), which prefers linear coordination and forms more stable metal−phosphorus bonds, restricts the nuclearity of the resulting complex to three. The trinuclear heterometallic complex [Cp*$_2$Zr{κ^1*O*-OOCC$_6$H$_4$-4-SAu(PMe$_2$Ph)}{κ^2*O,O′*-OOCC$_6$H$_4$-4-SAu(PMe$_2$Ph)}] (**3**) is stable in solution and is therefore more suitable than the rhodium(I) complex for investigation of its spectroscopic properties.

Experimental Section

General Details. Operations were performed under a dry nitrogen atmosphere using standard Schlenk techniques, except where otherwise stated. Solvents and reagents were purified by standard procedures. H$_2$mba was purchased from Aldrich and used without further purification. PMe$_2$Ph[12] and [Cp*$_2$ZrMe$_2$][13] (Cp* = C$_5$Me$_5$) were prepared according to literature procedures. NMR spectra were recorded with a Bruker AVANCE DRX 400 (^{1}H NMR 400.13 MHz, ^{13}C NMR 100.3 MHz, ^{31}P NMR 161.97 MHz) (Scheme 1). Si(CH$_3$)$_4$ was used as internal standard for the ^{1}H and ^{13}C NMR spectra. H$_3$PO$_4$ was used as external standard for the ^{31}P NMR spectra. IR spectra (KBr) were recorded on a Perkin-Elmer Spektrum 2000 FTIR spectrometer in the range 350−4000 cm^{-1}. The elemental composition was determined with a Hereaus CHN-O-S-Analyzer. Melting points were determined in sealed capillaries (under nitrogen) using a Gallenkamp apparatus and are uncorrected. UV/vis spectra were recorded with a Perkin-Elmer Lambda 900 UV/vis/NIR spectrometer. Photoluminescence (PL) experiments were performed with a Spex Fluorolog-3 spectrometer. Crystals of **1** were dispersed in a viscous polyfluoroether oil (ABCR), layered between two 1 mm thick quartz plates and mounted on a coldfinger of an optical closed-cycle cryostat (Leybold) operating at 15−293 K. All emission spectra were corrected for the wavelength-dependent response of the spectrometer. The PL quantum yield of **1** in the solid state was evaluated according to a procedure described elsewhere.[14]

Scheme 1. Numbering Scheme for the Assignment of the NMR Signals of the Aromatic Rings

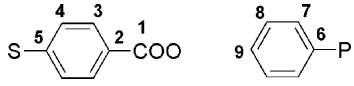

[Au(SC$_6$H$_4$-4-COOH)(PMe$_2$Ph)] (1). H[AuCl$_4$]·3H$_2$O (0.39 g, 1.00 mmol) was dissolved in distilled water (5 mL). A solution of S(CH$_2$CH$_2$OH)$_2$ (0.24 g, 2.00 mmol) in distilled water (10 mL) was added quickly. After decolorization (a few seconds) of the yellow solution, a solution of 4-mercaptobenzoic acid (0.15 g, 1.00 mmol) in ethanol (25 mL) was added, and a light yellow solid immediately precipitated. After 5 min of stirring at room temperature, the solid [Au(SC$_6$H$_4$-4-COOH)] was filtered off, washed three times with water and ethanol, and dried under vacuum. All these steps can be carried out in air without any precautions regarding exclusion of oxygen or water. Yield: 0.32 g (91%). Anal. Calcd for C$_7$H$_5$O$_2$SAu (350.1): C, 24.01; H, 1.44. Found: C, 23.37; H, 1.38. IR (KBr pellet; $\tilde{\nu}$ (cm^{-1})): 2972 m, 2649 m, 2524 m, 2074 w, 1796 w (br), 1687 s (br), 1589 s, 1561 s, 1485 m, 1415 s, 1395 s (sh), 1301 m (br), 1272 s (br), 1228 s (br), 1173 s, 1124 m, 1105 m, 1078 m, 1043 m, 1012 s, 933 w (br), 868 w, 846 m, 790 m (sh), 758 s, 702 w, 682 m, 629 w, 545 m (br), 519 m (br), 476 m (sh), 430 w, 417 w, 404 w.

PMe$_2$Ph (0.12 mL, 0.92 mmol) was added to a suspension of [Au(SC$_6$H$_4$-4-COOH)] in thf (20 mL). Within a few minutes the solid dissolved yielding a pale yellow solution. All volatile compounds were evaporated in vacuum, and the resulting pale yellow solid was washed with *n*-hexane and recrystallized from thf to afford bright yellow needles. Yield: 0.42 g (93%). Mp (decomp) 193 °C. Anal. Calcd for C$_{15}$H$_{16}$O$_2$SPAu (488.27): C, 36.90; H, 3.30. Found: C, 36.46; H, 3.33. IR (KBr pellet; $\tilde{\nu}$ (cm^{-1})): 3440 m (br), 3053 w, 2963 m, 2906 w, 2664 w, 2550 w, 1689 s (sh), 1588 s, 1548 w, 1486 w, 1435 m, 1416 m (sh), 1313 m, 1290 m, 1261 s, 1224 w, 1177 m, 1089 s (br, sh), 1022 s (br), 952 w, 914 m, 867 w, 803 s (sh), 756 w, 743 m, 720 w, 694 m, 549 w, 525 w, 481 m (sh), 446 w. UV/vis (thf), λ_{max} (nm): 330. EI MS, *m/z*, rel. Int.: 488 [Au(SC$_6$H$_4$-4-COOH)(PMe$_2$Ph)], 1%; 368 [Me$_2$PhPAuS]$^+$, 1%; 335 [Me$_2$PhPAu]$^+$, 1%; 154 [HSC$_6$H$_4$COOH]$^+$, 17%; 138 [PhMe$_2$P]$^+$, 100%; 123 [PhMeP]$^+$, 92%; 107 [PhP-H]$^+$, 17%; 77 [Ph]$^+$, 22%. ^{1}H NMR ([D$_8$]thf, 25 °C): δ 1.89 (d, 6H, $^2J_{HP}$ = 12.0 Hz, P(C*H*$_3$)$_2$), 7.47 (d, 2H, $^3J_{HH}$ = 8.3 Hz, H4), 7.50 (m, 3H, H7, H9), 7.62 (d, 2H, $^3J_{HH}$ = 8.3 Hz, H3), 7.85 (m, 2H, H8), ca. 11.3 (broad, COO*H*). ^{13}C{^{1}H} NMR ([D$_8$]thf, 25 °C): δ 14.9 (d, $^1J_{CP}$ = 35.8 Hz, P(*C*H$_3$)$_2$), 125.6 (s, C5), 129.5 (s, C3), 129.7 (d, $^2J_{CP}$ = 11.2 Hz, C7), 132.0 (d, $^4J_{CP}$ = 2.3 Hz, C9), 132.2 (s, C4), 132.6 (d, $^3J_{CP}$ = 13.4 Hz, C8), 134.0 (d, $^1J_{CP}$ = 55.8 Hz, C6), 153.2 (s, C2), 167.6 (s, C1). ^{31}P{^{1}H} NMR ([D$_8$]thf, 25 °C): δ 10.0 (s, *P*Me$_2$Ph).

[Cp*$_2$Zr(κ^1*O*-O$_2$CC$_6$H$_4$-4-SH)(κ^2*O,O′*-O$_2$CC$_6$H$_4$-4-SH)] (2). 4-Mercaptobenzoic acid (0.18 mg, 1.2 mmol) was dissolved in thf (15 mL) and added to a solution of [Cp*$_2$ZrMe$_2$] (0.24 g, 0.6 mmol) in toluene (8 mL). Over the next ten minutes evolution of gas was observed, and the solution was stirred for 1 h at room temperature. The solution was concentrated to 2 mL, and the product precipitated with *n*-hexane (5 mL). Yield: 0.37 g (83%). Mp: 269 °C (decomp). Anal. Calcd for C$_{34}$H$_{40}$O$_4$S$_2$Zr (740.1): C, 61.7; H, 6.5. Found: C, 61.2; H, 6.4. IR (KBr pellets, $\tilde{\nu}$ (cm^{-1})): 3062 m, 2957 s, 2905 s, 2726 w, 2488 m, 2033 w, 1920 w, 1802 w, 1687 w, 1618 s (sh 1635 s), 1594 s, 1580 s, 1559 m, 1518 s, 1498 s, 1446 s, 1397 m, 1379 s, 1363 m, 1330 s (sh 1325 s), 1279 w, 1260 m, 1238 w, 1176 m, 1140 s, 1098 s, 1016 s, 956 w, 915 w, 872 s, 845 s, 805 s, 763 s, 734 m, 717 w, 689 m, 631 w, 612 w, 593 w, 542 s, 516 s, 471 m. FAB MS, *m/z*, rel. int.: 531 [Cp*Zr(OOCC$_6$H$_4$S)$_2$]$^+$, 100%; 513 [Cp*$_2$Zr(OOCC$_6$H$_4$S)]$^+$, 82%; 395 [Cp*$_2$ZrOO + H]$^+$, 18%; 377 [Cp*$_2$ZrO + H]$^+$, 17%. ^{1}H NMR (C$_6$D$_6$, 25 °C): δ 1.86 (s, 30 H, C$_5$(C*H*$_3$)$_5$), 3.08 (s, 2H, S*H*), 7.07 (d, 4H, $^3J_{HH}$ = 8.0 Hz, H4), 8.35 (d, 4H, $^3J_{HH}$ = 8.0 Hz, H3). ^{13}C{^{1}H} NMR (C$_6$D$_6$, 25 °C): δ 11.9 (s, C$_5$(*C*H$_3$)$_5$), 122.9 (s, C4, *C*$_5$(CH$_3$)$_5$), 131.4 (s, C3), 132.7 (s, C5), 137.9 (s, C2), 174.1 (s, C1).

(10) Helmstedt, U.; Lönnecke, P.; Hey-Hawkins, E. *Inorg. Chem.* **2006**, *45*, 10300–10308.
(11) Helmstedt, U.; Lönnecke, P.; Reinhold, J.; Hey-Hawkins, E. *Eur. J. Inorg. Chem.* **2006**, 4922–4930.
(12) Meisenheimer, J.; Casper, J.; Höring, M.; Lauter, W.; Lichtenstadt, L.; Samuel, W. *Liebigs Ann. Chem.* **1926**, *449*, 213–248.
(13) (a) Manriquez, J. M.; Bercaw, J. E. *J. Am. Chem. Soc.* **1974**, *96*, 6229–6230. (b) Manriquez, J. M.; McAllister, D. R.; Rosenberg, E.; Shiller, A. M.; Williamson, K. L.; Chan, S. I.; Bercaw, J. E. *J. Am. Chem. Soc.* **1978**, *100*, 3078–3083. (c) Manriquez, J. M.; McAllister, D. R.; Sanner, R. D.; Bercaw, J. E. *J. Am. Chem. Soc.* **1978**, *100*, 2716–2724.
(14) Lebedkin, S.; Langetepe, T.; Sevillano, P.; Fenske, D.; Kappes, M. M. *J. Phys. Chem. B* **2002**, *106*, 9019–9026.

Table 1. Crystallographic Data for **1**, **2**·thf, and **4**

	1	**2**	**4**
empirical formula	$C_{15}H_{16}AuO_2PS$	$C_{38}H_{48}O_5S_2Zr$	$C_{36}H_{48}AuO_2PSZr$
M_r	488.27	740.10	863.96
T [K]	293(2)	293(2)	293(2)
crystal system	orthorhombic	monoclinic	triclinic
space group	*Ccc*2	$P2_1/c$	$P\bar{1}$
a [pm]	1580.4(2)	983.3(1)	868.05(8)
b [pm]	2829.1(4)	2617.9(3)	925.18(9)
c [pm]	698.35(8)	1392.6(1)	2467.2(2)
α [°]	90	90	82.721(2)
β [°]	90	92.203(2)	82.930(2)
γ [°]	90	90	65.086(2)
V [nm^3]	3.1224(7)	3.5822(6)	1.7772(3)
Z	8	4	2
$\rho_{calcd.}$ [g cm^{-3}]	2.077	1.372	1.615
μ [mm^{-1}]	9.657	0.465	4.549
$F(000)$	1856	1552	860
crystal size [mm]	0.40 × 0.20 × 0.10	0.60 × 0.30 × 0.20	0.20 × 0.20 × 0.10
θ range [°]	1.44−28.28	1.56−28.94	2.50−28.96
h,k,l collected	$-20 \le h \le 13$	$-8 \le h \le 13$	$-11 \le h \le 9$
	$-37 \le k \le 36$	$-32 \le k \le 35$	$-11 \le k \le 11$
	$-8 \le l \le 9$	$-18 \le l \le 17$	$-33 \le l \le 17$
measured reflections	9524	22946	11482
unique reflections	3639	8702	8225
restraints/parameters	1/185	0/433	0/392
GoF (all data)	1.092	1.075	1.016
final R indices	$R_1 = 0.0324$	$R_1 = 0.0396$	$R_1 = 0.0414$
$[I > 2\sigma(I)]$	$wR_2 = 0.0793$	$wR_2 = 0.1074$	$wR_2 = 0.0968$
R indices	$R_1 = 0.0598$	$R_1 = 0.0624$	$R_1 = 0.0586$
(all data)	$wR_2 = 0.1097$	$wR_2 = 0.1202$	$wR_2 = 0.1062$
$\Delta\rho$ (max/min) [e Å^{-3}]	0.828/−1.198	0.852/−0.492	2.205/−1.918
absolute structure parameter	0.16(2) (refined as racemic twin)		

Scheme 2

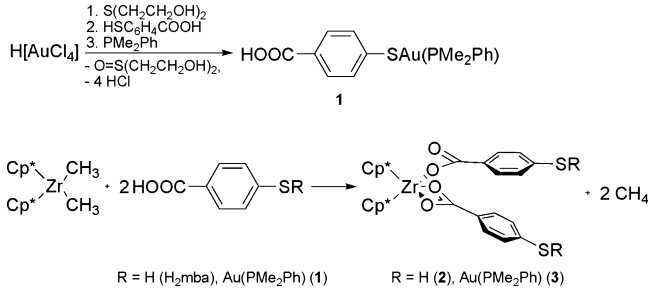

[Cp*$_2$Zr{κ^1*O*-O$_2$CC$_6$H$_4$-4-SAu(PMe$_2$Ph)}{κ^2*O,O′*-O$_2$CC$_6$H$_4$-4-SAu(PMe$_2$Ph)}] (3). A solution of **1** (0.29 g, 0.6 mmol) in thf (15 mL) was added at room temperature to a solution of [Cp*$_2$ZrMe$_2$] (0.12 g, 0.3 mmol) in toluene (5 mL). Gas evolution was observed, and the solution was stirred for 30 min. The solution was reduced to a volume of about 5 mL, and the colorless product precipitated by addition of *n*-hexane (20 mL). Yield: 0.28 g (69%). Anal. Calcd for $C_{50}H_{60}O_4P_2S_2Au_2Zr$ (1336.2): C, 44.94; H, 4.53. Found: C, 44.68; H, 4.39. IR (KBr pellets, $\tilde{\nu}$ (cm^{-1})): 3051 w, 2963 s, 2904 m, 2541 w, 1879 w, 1704 w, 1614 m (sh at 1625 s), 1586 s, 1545 m, 1496 m, 1427 s, 1380 m, 1313 s (sh at 1335 s), 1261 s, 1171 m, 1138 m, 1084 s, 1024 s, 951 m, 912 s, 872 m, 845 m, 802 s, 774 m, 742 m, 719 w, 692 m, 632 w, 595 w, 547 m, 520 m, 482 m, 444 m. UV/vis (thf), λ_{max} (nm): 336. FAB MS, *m*/*z*, rel. Int.: 1334 [Cp*$_2$Zr{O$_2$CC$_6$H$_4$-4-SAu(PMe$_2$Ph)}$_2$ + H]$^+$, 2%; 1257 [Cp*$_2$Zr{O$_2$CC$_6$H$_4$-4-SAu(PMe$_2$Ph)}{O$_2$CC$_6$H$_4$-4-SAu(PMe$_2$)}]$^+$, 3%; 847 [Cp*$_2$Zr{O$_2$CC$_6$H$_4$-4-SAu(PMe$_2$Ph)}]$^+$, 95%; 513 [Cp*$_2$Zr(O$_2$CC$_6$H$_4$-4-S)+H]$^+$, 40%; 488 [O$_2$CC$_6$H$_4$-4-SAu(PMe$_2$Ph) + H]$^+$, 28%; 335 [Au(PMe$_2$Ph)]$^+$, 100%. ^{1}H NMR (CDCl$_3$, 25 °C): δ 1.85 (s, 30H, C$_5$(C*H*$_3$)$_5$), 1.86 (d, 12H, $^2J_{HP}$ = 8.0 Hz, P(C*H*$_3$)$_2$), 7.51 (m, 6H, H7, H9), 7.62 (d, 4H, $^3J_{HH}$ = 8.0 Hz, H4), 7.76 (m, 4H, H8), 8.00 (d, 4H, $^3J_{HH}$ = 8.0 Hz, H3). ^{13}C{^{1}H} NMR (CDCl$_3$, 25 °C): δ 11.8 (s, C$_5$(*C*H$_3$)$_5$), 16.4 (d, $^1J_{CP}$ = 35.3 Hz, P(*C*H$_3$)$_2$), 122.1 (s, *C*$_5$(CH$_3$)$_5$), 129.8−130.4 (m, C7, C9, C4, C5), 132.4 (s, C3), 132.6 (d, $^3J_{CP}$ = 13.0 Hz, C8), 132.8 (d, $^1J_{CP}$ = 49.6 Hz, C6), 149.1 (s, C2), 175.1 (s, C1). ^{31}P{^{1}H} NMR (CDCl$_3$, 25 °C): δ 12.7 (s, PMe$_2$Ph).

[Cp*$_2$Zr(Me){κ^2*O,O′*-OOCC$_6$H$_4$-4-SAu(PMe$_2$Ph)}] (4). A few crystals of **4** could be isolated from a crystallization trial for **3**.

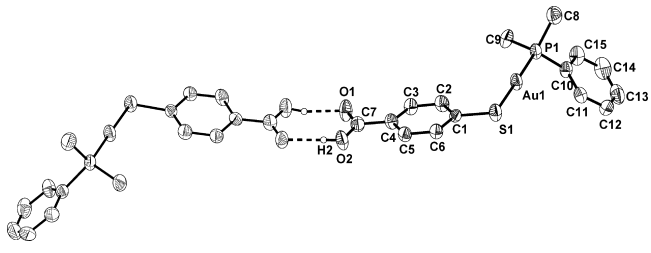

Figure 1. Hydrogen-bonded dimer of **1** (50% thermal ellipsoids). Hydrogen atoms bonded to carbon have been omitted. Selected bond lengths (Å) and angles (°): Au(1)−P(1) 2.266(2); Au(1)−S(1) 2.313(2); O(1)−C(7) 1.26(1); O(2)−C(7) 1.26(1); P(1)−Au(1)−S(1) 178.91(7); O(1)−C(7)−O(2) 123(1); distance between hydrogen-bridged oxygen atoms = 2.61.

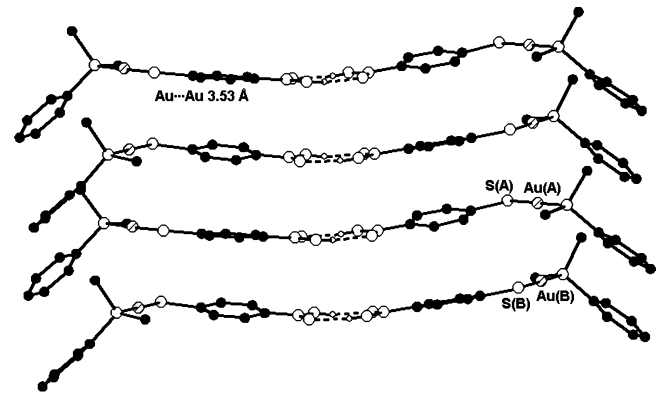

Figure 2. Side view of a stack of hydrogen-bonded dimers of **1**.

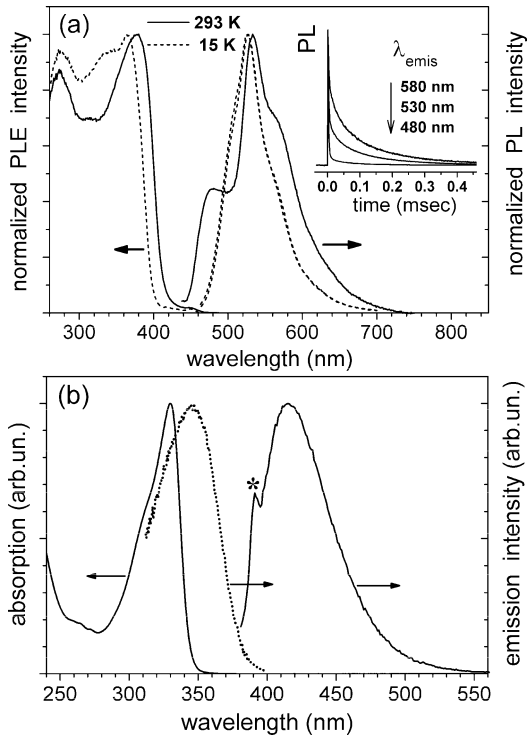

Figure 3. (a) Normalized PLE and emission PL spectra of crystals of **1** at temperatures of 293 and 15 K. The emission wavelength for PLE spectra is 530 nm, the excitation wavelengths for PL spectra are 350 nm (293 K) and 280 and 350 nm (15 K). The latter spectra coincide, illustrating that the PL is independent of excitation wavelength. The inset shows normalized decay curves of the PL excited with an N_2 laser (337 nm, ca. 4 ns pulses) and recorded at different emission wavelengths at 293 K. (b) Normalized absorption, PLE, and emission PL spectra of a thf solution of **1** at 293 K. The excitation and emission wavelengths for PL and PLE spectra are 350 and 420 nm, respectively. The asterisk indicates a Raman band of the solvent. Arrows indicate affiliation to the different axes.

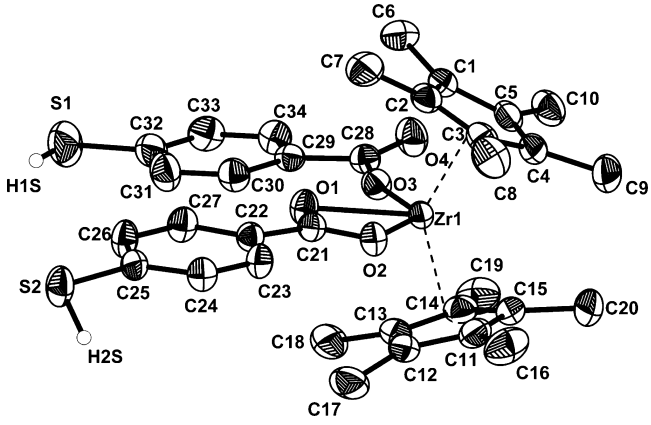

Figure 4. Molecular structure of **2** (50% thermal ellipsoids). Hydrogen atoms bonded to carbon have been omitted. Selected bond lengths (Å) and angles (°): Zr(1)−O(1) 2.273(2); Zr(1)−O(2) 2.305(2); Zr(1)−O(3) 2.083(2); O(4)−C(28) 1.227(3); C(21)−O(1)−Zr(1) 93.3(1); C(21)−O(2)−Zr(1) 92.2(1); C(28)−O(3)−Zr(1) 165.0(2); O(2)−C(21)−O(1) 117.8(2); O(1)−Zr(1)−O(2) 56.72(6); O(4)−C(28)−O(3) 123.9(2).

FAB MS, *m*/*z*, rel. Int.: 862 $[Cp^*_2Zr(CH_3)\{OOCC_6H_4\text{-}4\text{-}SAu(PMe_2Ph)\} + H]^+$, 20%; 847 $[Cp^*_2Zr\{OOCC_6H_4\text{-}4\text{-}SAu(PMe_2Ph)\}]^+$, 25%; 513 $([Cp^*_2Zr(OOCC_6H_4S) + H]^+$, 16%; 335 $[PhMe_2PAu]^+$, 100%. ^{1}H NMR ($CDCl_3$, 25 °C): δ 0.07 (s, 3H, $ZrCH_3$), 1.84 (s, 15H, $C_5(CH_3)_5$), 1.86 (s, 15H, $C_5(CH_3)_5$), 1.87 (d, 6H, $^2J_{HP}$ = 8.3 Hz, $P(CH_3)_2$)), 7.53 (m, 3H, H7, H9), 7.61 (d, 2H, $^3J_{HH}$ = 8.3 Hz, H4), 7.78 (m, 2H, H8), 7.81 (d, 2H, $^3J_{HH}$ = 8.3 Hz, H3). The isolated amount of the substance was not sufficient to measure $^{13}C\{^1H\}$ NMR spectra. $^{31}P\{^1H\}$ NMR ($CDCl_3$, 25 °C): δ 11.6 (s, PMe_2Ph).

X-ray Crystallography. X-ray data were collected with a Siemens CCD Smart diffractometer using graphite-monochromated Mo Kα radiation (λ = 0.71073 Å). Absorption correction was performed with the program SADABS.[15] The space groups were determined with XPREP.[16] Structure solution and refinement were performed with WINGX,[17] SHELXS-97, and SHELXL-97.[18] All non-hydrogen atoms were refined anisotropically; most hydrogen atoms were refined in calculated positions. Visualization was carried out with the program DIAMOND. The crystallographic data are summarized in Table 1. CCDC-668319 (**1**), CCDC-668321 (**2**), and CCDC-668320 (**4**) contain the supplementary crystallographic data for this paper. These data can be obtained free of charge from Cambridge Crystallographic Data Centre via www.ccdc.cam.ac.uk/data_request/cif.

Results and Discussion

Synthesis. The gold(I) thiolato complex of 4-mercaptobenzoic acid could be easily obtained by reduction of tetrachloroaurate with bis(hydroxyethyl) sulfide[19] followed by treatment with 4-mercaptobenzoic acid. A suspension of the resulting colorless solid was treated with dimethylphenylphosphine to produce $[Au(SC_6H_4\text{-}4\text{-}COOH)(PMe_2Ph)]$ (**1**) in nearly quantitative yield (Scheme 2). The zirconocene biscarboxylato complexes $[Cp^*_2Zr(\kappa^1O\text{-}O_2CC_6H_4\text{-}4\text{-}SR)(\kappa^2O,O'\text{-}O_2CC_6H_4\text{-}4\text{-}SR)]$ [R = H (**2**), $Au(PMe_2Ph)$ (**3**)] could be obtained by methane elimination starting from $[Cp^*_2ZrMe_2]$ and 2 equiv of the corresponding carboxylic acid (H_2mba for **2**, and **1** for **3**; Scheme 2). Methane elimination occurs readily and purification is simple.

Structure and Spectroscopic Properties. $[Au(SC_6H_4\text{-}4\text{-}COOH)(PMe_2Ph)]$ (1). Bright yellow needles of **1** were obtained by crystallization from thf and structurally characterized (Figure 1).

Compound **1** crystallizes in the orthorhombic space group *Ccc*2 with eight molecules in the unit cell. As expected the gold atom is coordinated by sulfur and phosphorus in a linear fashion with an S−Au−P bond angle of 178.91°. The molecules are planar with the exception of the substituents at the phosphorus atom and form dimers by hydrogen bonding between the carboxyl groups, as shown in Figure 1. The molecule has a chiral axis in the solid state marked by the atoms S, Au and P (see Supporting Information), and one dimer consists of molecules with the same chirality. These dimers build stacks with alternating pairs of *R* and *S* enantiomers (Figure 2). Viewed down the stacks the S(A)−Au(A)···Au(B)−S(B) dihedral angle is 121.2°.

The distance between two gold atoms in the stack is 3.534 Å. The linear relationship between gold−gold distances and

(15) Sheldrick, G. M.; *SADABS, A Program for Empirical Absorption Correction*; University of Göttingen: Göttingen, Germany, 1998.
(16) Bruker, *XPREP in SHELXTL version 6.12*; Bruker AXS Inc.: Madison, WI, 2002.
(17) Farrugia, L. J. *WINGX, Suite for Small-Molecule Single-Crystal Crystallography*; *J. Appl. Crystallogr.* **1999**, *32*, 837−838.
(18) Sheldrick, G. M. *SHELXS97, SHELXL97, Programs for Crystal Structure Analysis*, Release 97−2; University of Göttingen: Göttingen, Germany, 1998.
(19) Al-Sa′ady, A. K. H.; Moss, K.; McAuliffe, C. A.; Parish, R. V. *J. Chem. Soc., Dalton Trans.* **1984**, 1609–1616.

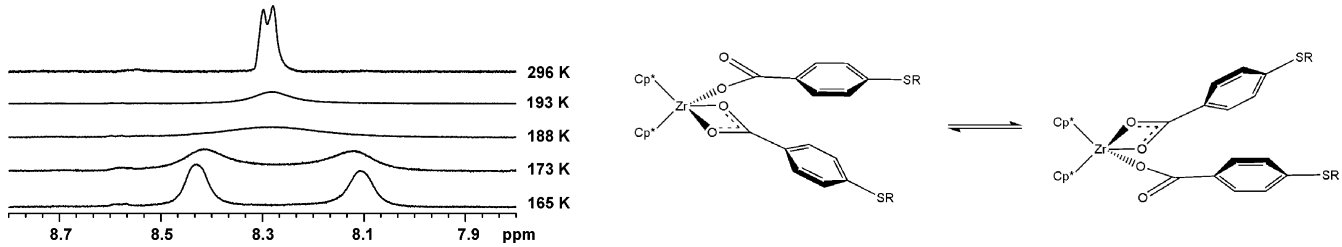

Figure 5. VT ^{1}H NMR signal of the proton in the position *ortho* to the carboxylato group (solution of **2** in [D_8]THF).

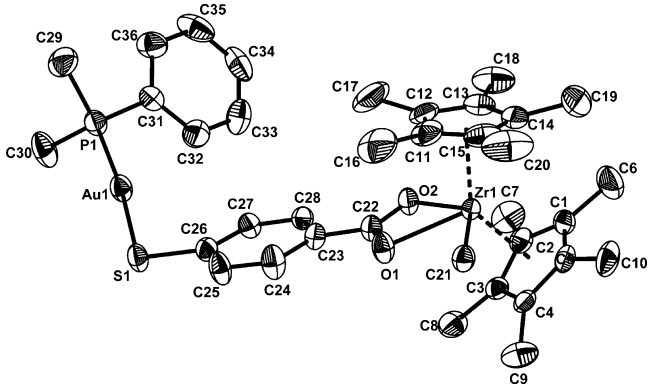

Figure 6. Molecular structure of **4** (50% thermal ellipsoids). Hydrogen atoms have been omitted. Selected bond lengths (Å) and angles (°): Zr(1)−O(1) 2.293(4); Zr(1)−O(2) 2.309(3); Zr(1)−C(21) 2.321(5); O(1)−C(22) 1.275(6); O(2)−C(22) 1.262(6); Au(1)−P(1) 2.255(1); Au(1)−S(1) 2.301(1); O(1)−Zr(1)−O(2) 56.7(1); O(1)−Zr(1)−C(21) 73.4(2); O(2)−Zr(1)−C(21) 123.0(2); O(2)−C(22)−O(1) 118.9(4); P(1)−Au(1)−S(1) 174.13(5).

the corresponding stabilization energy was quantitatively described by Schwerdtfeger[20] and Pyykkö.[21] Both theoretical investigations yield stabilizing energies of around 10 kJ mol^{-1} for this distance. Despite this small gain in energy, repetitive addition of these amounts along the chain might contribute to the stability of this arrangement of molecules. Moreover, the intermolecular (aurophilic) interactions might explain dramatic differences in the PL properties of crystalline **1** as compared to a solution (see below). In the corresponding (triphenylphosphine)gold(I) complex of 4-mercaptobenzoic acid,[22] the same structural motif of dimers as shown in Figure 1 is observed. In contrast to **1**, the higher steric bulk of three phenyl rings at the phosphorus atom prevents formation of stacks, but dimeric structures are formed via strong aurophilic interactions.

Figure 3a shows the PL excitation (PLE) and emission spectra of crystals of **1** at ambient and low temperatures. The emission spectra are structured (better seen at ambient temperature), with at least three components (at ca. 478, 533, and 570 nm at 293 K). Similar PLE and PL spectra were recorded at emission and excitation wavelengths between 480 and 580 nm and 280 and 400 nm, respectively, that is, the PL is practically independent of the excitation wavelength. On the other hand, the PL kinetics (inset in Figure 3) are complex and depend on the emission wavelength. They can be approximately described by two exponential components with characteristic times of a few and hundreds of microseconds, respectively. The fast component corresponds mainly to the PL band at about 478 nm, whereas the slow component corresponds to the red-shifted PL bands at about 530−580 nm. The latter demonstrate an unusually long lifetime, which increases to about 0.5 ms on decreasing the temperature to 15 K. We tentatively attribute the multiple emission to several weakly coupled radiative relaxation channels in **1**, including different metal-centered (^{1}MC and ^{3}MC) and ligand-to-metal charge-transfer excited states, in line with assignments for other gold(I) complexes.[23] Relative efficiencies of these channels depend on the temperature as indicated by changes in the emission spectra.

The PL of solid **1** is bright and in fact responsible for the brilliant yellow color of this compound (note that the PLE spectrum indicates the absorption edge at ca. 420 nm; see Figure 3a). The PL quantum yield φ_{PL} was estimated to be as high as 0.2−0.3 at 293 K. In parallel with the slowing of the PL decay, the PL intensity uniformly increases with decreasing the temperature down to ∼100 K. At the lower temperatures, φ_{PL} does not change significantly and approaches ∼0.7−1 at $T \approx$ 15 K. In contrast to the solid sample, a solution of **1** in thf shows a weak single PL band at 415 nm (Figure 3b). The PLE spectrum (dotted line) is significantly red-shifted relative to the first absorption band of **1**, likely indicating that a weakly absorbing MC state, not ligand excitations, mostly contributes to the PL of **1** in solution. These observations suggest quite different electronic relaxation patterns in crystalline **1** versus "monomers" of **1** in solution.

Complex **1** is soluble in thf, and dissolution of **1** in other organic solvents such as benzene and toluene could only be achieved by addition of thf. The chemical shifts of the protons of the aromatic rings show solvent dependence (±0.2 ppm in thf compared to C_6D_6) for **1** as well as for compounds **2** and **3** (see Supporting Information). The reason for this phenomenon, known as "aromatic solvent induced shift" (ASIS),[24] is probably weak interactions between the aromatic rings of **1**−**3** and the solvent molecules.

[Cp*$_2$Zr(κ^1*O*-O$_2$CC$_6$H$_4$-4-SH)(κ^2*O,O′*-O$_2$CC$_6$H$_4$-4-SH)] (2). Suitable crystals of **2** for X-ray structure analysis were obtained from a mixture of thf and *n*-hexane; **2** crystallizes as needles in the monoclinic space group $P2_1/c$ with four molecules of **2** and four molecules of thf in the unit cell (Figure 4).

One of the ligands is coordinated in a bidentate and the other in a monodentate fashion to the zirconium atom. With one

(20) Schwerdtfeger, P.; Bruce, A. E.; Bruce, M. R. M. *J. Am. Chem. Soc.* **1998**, *120*, 6587–6597.
(21) Pyykkö, P. *Angew. Chem., Int. Ed.* **2004**, *43*, 4412–4456.
(22) Wilton-Ely, J. D. E. T.; Schier, A.; Mitzel, N. W.; Schmidbaur, H. *J. Chem. Soc., Dalton Trans.* **2001**, 1058–1062.
(23) Lee, Y.-A.; McGarrah, J. E.; Lachicotte, R. J.; Eisenberg, R. *J. Am. Chem. Soc.* **2002**, *124*, 10662–10663.
(24) (a) Braun, S.; Kalinowski, H.-O.; Berger, S. *150 and more NMR-Experiments*; Wiley VCH: New York, 1998. (b) Stamm, H.; Jäckel, H. *J. Am. Chem. Soc.* **1989**, *111*, 6544–6550.

Table 2. Comparison of Selected NMR, IR and UV/vis Spectroscopic Data of **1**, **2**, and **3**

compound	$\delta(^{31}P)^a$	$\delta(^{13}C)$ (Cp*)^a	$\delta(^{13}C)$ (PCH_3/PC_6H_5, *ipso-C*)^a	$\tilde{\nu}$ (C=O)^b	$\lambda_{max}{}^c$
1	10.0		14.9/134.0		330 nm
2		122.8		1618 cm^{-1}	
3	12.7	122.1	16.4/132.8	1614 cm^{-1}	336 nm

^{a} Solution in [D_8]thf. ^{b} KBr pellet;. ^{c} Solution in thf.

exception, namely, $[Cp^*_2Zr(OCOCF_3)_2]$,[25] this bonding mode has always been observed for zirconocene bis-carboxylato complexes.[9,26] As expected for a delocalized π system, the O(1)−C(21) and O(2)−C(21) bond lengths are nearly equal. The different bonding modes of the ligands are also reflected in the IR spectrum by the occurrence of four strong bands: two for the C=O and C−O stretching modes of the monodentate ligand at 1635 and 1176 cm^{-1}, respectively, and two for the symmetric and antisymmetric stretching modes of the bidentate ligand at 1559 cm^{-1} and 1325 cm^{-1}. These values are in good agreement with previously reported frequencies for zirconocene bis-carboxylato complexes.[9b,26d]

In contrast to the solid-state structure, the ^1H NMR spectrum of **2** shows only one set of signals for the aromatic rings. The equivalency of the ligands in solution is caused by a fast exchange of the two ligands between mono- and bidentate bonding, as could be shown by variable-temperature NMR spectroscopy (Figure 5). The doublet of the proton in the position *ortho* to the carboxylato group splits into two signals at low temperature (coalescence temperature 175 K), while the signal of the proton in the *meta* position remains nearly unchanged.

The thermodynamic parameters were determined by line shape analysis, which gave an activation energy $\Delta G^{\ddagger}$ (298 K) of 40.6 kJ mol^{-1} with an activation enthalpy $\Delta H^{\ddagger}$ of 24 kJ mol^{-1} and an activation entropy $\Delta S^{\ddagger}$ of −55.6 J K^{-1} mol^{-1}. To the best of our knowledge **2** is the first zirconocene bis-carboxylato complex for which coalescence was observed by NMR spectroscopy. Generally, no changes were observed down to 180 K (restricted by the freezing point of the solvent).[9,26e]

$[Cp^*_2Zr\{\kappa^1O\text{-}OOCC_6H_4\text{-}4\text{-}SAu(PMe_2Ph)\}\{\kappa^2O,O'\text{-}OOCC_6H_4\text{-}4\text{-}SAu(PMe_2Ph)\}]$ (3). Two equivalents of **1** react with $[Cp^*_2ZrMe_2]$ at room temperature with nearly quantitative formation of the trinuclear complex $[Cp^*_2Zr\{OOCC_6H_4\text{-}4\text{-}SAu(PMe_2Ph)\}_2]$ (**3**; Scheme 2). As observed for **2**, the IR spectrum of **3** exhibits four strong bands at 1625, 1171 cm^{-1} and 1545, 1335 cm^{-1}, which correspond to the different bonding modes of the carboxylato ligands. On cooling, the signal of the hydrogen atoms *ortho* to the carboxylato group broadens and splits into two signals between 190 and 200 K. Because of overlap of these signals with those of the aromatic protons of the PMe_2Ph group, line shape analysis could not be carried out. The coalescence temperature is nevertheless higher for **3** than for **2**. This might be due to increased steric hindrance in the bulky trinuclear complex, which hinders this process.

A few colorless crystals of the byproduct $[Cp^*_2Zr(Me)\{\kappa^2O,O'\text{-}OOCC_6H_4\text{-}4\text{-}SAu(PMe_2Ph)\}]$ crystallized from the mother liquor after isolation of **3**. Compound **4** crystallizes in the triclinic space group $P\bar{1}$ with two molecules in the unit cell. The molecular structure is shown in Figure 6. An 18-valence-electron zirconocene complex results because of bidentate coordination of the carboxylato group. Zr(1), O(1), O(2), and C(21) are coplanar.

Linear coordination by sulfur and phosphorus is observed for Au(1) (S−Au−P 174.13°). In contrast to **1** the gold atom deviates from the S-phenylene plane; the torsion angle C(27)−C(26)−S(1)−Au(1) is 28.4° (corresponding torsion angle for **1**: 4.2°).

To study metal−metal interactions, relevant spectroscopic properties of **1** and **2** were compared with those of the heterometallic complex **3**. The chemical shifts of the phosphorus atom and the P−C carbon atoms (P−Me and P−Ph) and the peak maxima of the lowest energy UV/vis absorption bands of **1** and **3** as well as the chemical shift of the Cp* carbon atoms and the wavenumbers of the C=O stretching vibrations of the monodentate ligand in **2** and **3** were almost identical, that is, M−M interaction is negligible (Table 2).

Conclusion

A rare example of a heterobimetallic Au^I/Zr^{IV} complex and its corresponding mononuclear complexes are described. According to UV/vis, IR, and NMR spectroscopy the Au···Zr interaction is negligible. The mononuclear complex $[Au(SC_6H_4\text{-}4\text{-}COOH)(PMe_2Ph)]$ (**1**) shows interesting photoluminescence properties, such as high quantum yield and unusually long characteristic decay times. $[Cp^*_2Zr(\kappa^1O\text{-}O_2CC_6H_4\text{-}4\text{-}SH)(\kappa^2O,O'\text{-}O_2CC_6H_4\text{-}4\text{-}SH)]$ (**2**) is the first zirconocene bis-carboxylato complex for which activation parameters for the dynamic mono- and bidentate coordination modes could be obtained.

Acknowledgment. U.H. thanks the Studienstiftung des Deutschen Volkes for a PhD grant. Support from the Graduiertenkolleg 378 (DFG) and a generous donation of $H[AuCl_4]$ from Umicore AG & Co KG are gratefully acknowledged.

Supporting Information Available: Data for solvent dependence of the ^1H NMR spectra of the compounds and the analysis of the variable-temperature NMR data (PDF). This material is available free of charge via the Internet at http://pubs.acs.org.

IC800203Y

(25) Dorn, H.; Shah, S. A. A.; Parisini, E.; Noltemeyer, M.; Schmidt, H.-G.; Roesky, H. W. *Inorg. Chem.* **1996**, *35*, 7181–7184.

(26) See, for example, (a) Gau, H.-M.; Chen, C. T.; Jong, T. T.; Chien, M.-Y. *J. Organomet. Chem.* **1993**, *448*, 99–106. (b) Thewalt, U.; Güthner, T. *J. Organomet. Chem.* **1989**, *361*, 309–317. (c) Howard, W. A.; Trnka, T. M.; Waters, M.; Parkin, G. *J. Organomet. Chem.* **1997**, *528*, 95–121. (d) Gau, H. M.; Schei, C. C.; Liu, L. K.; Luh, L. H. *J. Organomet. Chem.* **1992**, *435*, 43–53. (e) Suzuki, H.; Takiguchi, T.; Kawasaki, Y. *Bull. Chem. Soc. Jpn.* **1978**, *51*, 1764–1767.